

Extreme precipitation events in Novi Sad during the period 1961-2020

Ivana Tošić^{A*}, Antonio Samuel Alves da Silva^B, Lazar Filipović^A, Suzana Putniković^A,
Tatjana Stosic^B, Borko Stosic^B, Vladimir Đurđević^A

^A Institute of Meteorology, Faculty of Physics, University of Belgrade, Belgrade, Serbia;
ORCID IT: 0000-0002-7259-8828, LF: 0009-0000-8209-4351, SP: 0000-0003-4930-6177

^B Department of Statistics and Informatics, Federal Rural University of Pernambuco, Rua
Dom Manoel de Medeiros s/n, Dois Irmãos, 52171-900 Recife, PE, Brazil; ORCID
ASAdS: 0000-0002-8759-0036, TS: 0000-0002-5691-945X; BS: 0000-0001-5031-6968

Received: March 11, 2025 | Revised: September 12, 2025 | Accepted: September 17, 2025

doi: 10.5937/gp29-57395

Abstract

Extreme precipitation events (EXPEs) were analyzed based on daily precipitation data from 1961 to 2020 in Novi Sad, Serbia. The temporal characteristics of the following EXPEs were investigated: Heavy precipitation days (R10mm), Very heavy precipitation days (R20mm), Highest 1-day precipitation amount (Rx1day), Highest 3-day precipitation amount (Rx3day), Highest 5-day precipitation amount (Rx5day), Very wet days (R95p), Extremely wet days (R99p), Precipitation fraction due to very wet days (R95pTot) and Precipitation fraction due to extremely wet days (R99pTot). The EXPEs were analyzed on an annual and seasonal basis and for two reference periods 1961-1990 and 1991-2020. Positive trends were found for both annual and seasonal values for all indices, except for R20mm and R99pTot in winter. A significant increase in Rx1day, Rx3day and Rx5day was observed in all seasons (except for Rx1day and Rx5day in winter) and on an annual basis. The high value of Rx1day (116.6 mm) was recorded in the summer of 2018 in Novi Sad, caused by convective precipitation that led to urban flooding. The possible influence of large-scale circulation patterns was investigated. A strong positive and negative influence of the East Atlantic pattern and the East Atlantic Western Russia pattern on the EXPEs was found. The results of this work support the growing evidence that the impact of extreme conditions is likely to become even stronger due to changes in their intensity and frequency.

Keywords: extreme precipitation events; precipitation indices; Novi Sad; Serbia

Introduction

The risk of extreme precipitation events is increasing due to global warming (e.g. Fuentes-Franco et al., 2023). It is known that a warmer atmosphere can hold more moisture (Zeder & Fisher, 2020). According to the Clausius-Clapeyron relationship, the intensity of daily extreme precipitation increases by about 7 % per °C temperature (Trenberth, 1999). There is a high confidence that extreme precipitation will increase with climate change (IPCC, 2021). A significant increase in heavy rainfall events has been observed worldwide, both on a continental and global scale (Westra et al., 2013; Sun et al., 2021) and on a regional scale (Wang et al., 2014). Van den Besselaar et al. (2013) found that five-, ten- and twenty-year

* Corresponding author: Ivana Tošić; itosic@ff.bg.ac.rs

events with 1-day and 5-day precipitation became more frequent in Europe in the period 1951–2010. Zeder and Fischer (2020) pointed out that extreme precipitation increased at the majority of stations in Central Europe in the period 1901–2013. Based on the daily precipitation from 40 regional climate simulations of the EURO-CORDEX ensemble, Etrichrätz et al. (2023) found a significant increase in heavy and extreme precipitation in Central, Northern and Eastern Europe. Extreme precipitation can lead to flooding (Berényi et al., 2023), soil erosion (Eekhout & de Vente, 2022), and landslides (Gariano & Guzzetti, 2016). Successful mitigation of these damages depends on the prediction of extreme rainfall events and better design and planning of urban drainage systems (Zhou et al., 2017; Davis & Naumann, 2017). Characterization of heavy rainfall events in urban areas is the first line of defense against urban flooding and crucial for risk management.

Serbia is a continental country in south-eastern Europe, located in the western region of the Balkan Peninsula. The northern part of the country is characterized by low elevation, which gradually rises towards the southern parts which are covered by mountains and hills surrounding river valleys. The climate of Serbia varies spatially from a temperate continental climate in the northern part to a continental climate in the central part and a modified Mediterranean climate in the southern part (Bajat et al., 2015). The average annual temperature in the lowlands is between 11 and 13 °C, while the average annual temperature in the mountains is below 8 °C. The mean annual precipitation is between 500 and 700 mm in the lowlands and over 1000 mm in the mountains (Vujadinović Mandić et al., 2022). The northern part of Serbia is the administrative unit of the Autonomous Province of Vojvodina, which is the most important agricultural region in the country. Agriculture is one of the most important sectors of the Serbian economy, and the factors that influence agriculture, especially climate conditions, have an impact on the economy of the entire country. Extreme weather conditions such as heavy precipitation affect not only crop production (Milošević et al., 2015; Mimić et al., 2022), but also the well-being of people living in urban areas. There are only a few recent studies that report the results of the analysis of precipitation in Vojvodina. Tošić et al. (2014) investigated the seasonal and annual variability of precipitation (recorded in monthly frequency at 92 stations in the period 1946–2006) in Vojvodina using empirical orthogonal functions (EOF). The trend analysis of the first EOF pattern (PC1) showed an increasing trend for annual, summer and fall precipitation and a decreasing trend for winter and spring precipitation. They indicated that the annual, winter and fall precipitation are influenced by the North Atlantic Oscillation (NAO).

Malinović-Milićević et al. (2018) examined the temporal and spatial variability of extreme precipitation in Vojvodina by analyzing the trends of extreme precipitation indices calculated from daily data from seven stations in the period 1966–2013. The results (based on precipitation magnitude and frequency) indicated that the climate is getting wetter in the northern and central part of the region, while the southernmost part of the region is getting drier, which is consistent with observations from central and southern European regions, respectively.

Bezdan et al. (2024) investigated the impact of climate change on extreme precipitation events and the associated risk of flooding based on the occurrence of the highest 3-day precipitation amount (Rx3day) in spring with a 10 years return period. They compared results from observational data (9 meteorological stations) for the period 1971–2019 with projections from 2020 to 2100 produced with an ensemble of eight regional climate models from the EURO-CORDEX project database. The results show that the Rx3day in spring increases by 19 to 33% with a 10 years return period and the probability of more than one event occurring in which the Rx3day exceeds the threshold values increases by 105.6 % to 200.0 % compared to the historical period. For the future period, the Rx3day values in spring

(used for the design of pluvial flood protection systems in Vojvodina) are below the future projections, indicating an increased risk of pluvial flooding.

In this work we focus on the extreme precipitation in the city of Novi Sad, the capital of Vojvodina. Previous studies dealt with the problem of heat waves (Savić et al., 2018) and heat islands (Unger et al., 2011) as well as dynamics of air temperature in the “local climate zones” (Milošević et al., 2022). The main objective of this study is to analyze extreme precipitation events (EXPEs) on an annual and seasonal basis from 1961 to 2020 in Novi Sad. We examined trend on annual and seasonal time series of all analyzed EXPE indices for the entire 60-year period and compared the descriptive statistics for the two 30-year reference periods (1961-1990 and 1991-2020). We also investigate the possible influence of large-scale circulation patterns on extreme precipitation.

Materials and Methods

Study area and data

Novi Sad is the capital of the autonomous province of Vojvodina and the second largest city in Serbia with 335,000 inhabitants and an area of 112 km² (Unger et al., 2011). Novi Sad is situated in the northern agricultural lowland region of Serbia, in the south of the Pannonian Plain (Fig. 1). The city center is surrounded by agricultural fields in the north, east and west (with a low elevation of about 80 m), while the southeastern districts of Sremska Kamenica and Petrovaradin are located on higher terrain (up to 130 m) on the edge of the northern slope of Fruška Gora (low mountain range with the highest peak at 539 m). The main watercourse is the Danube, which is 260-680 m wide and flows in the east-west direction in the southern part of the town. The Danube–Tisza–Danube Canal crosses the city from northwest to southeast and separates the industrial area in the north from the urban area in the south. The climate exhibits characteristics of the Cfb-Köppen–Geiger (temperate climate with warm summers and well-distributed precipitation throughout the year) climate type (Milošević et al., 2022). Based on data from 1949 to 2015, the mean annual precipitation is 622.8 mm and the mean monthly temperature ranges from -0.3 °C in January to 21.8 °C in July (Savić et al., 2018).

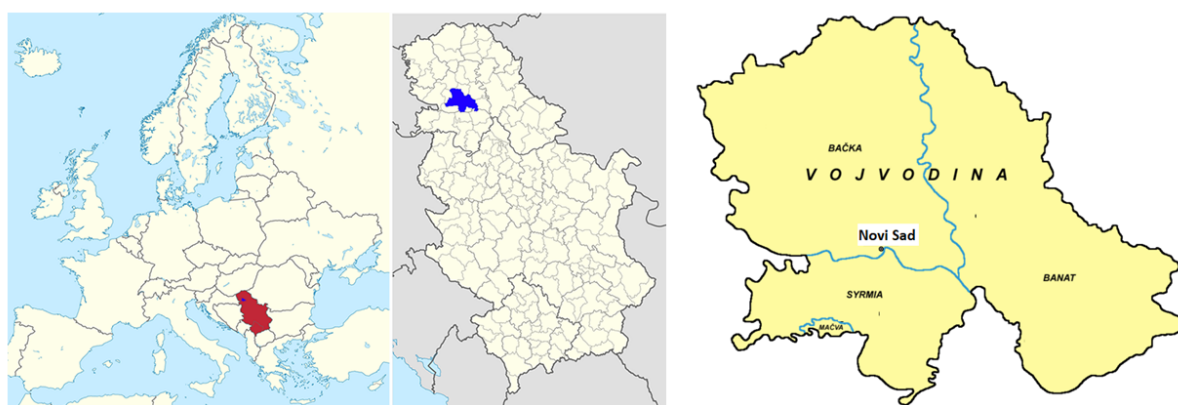


Figure 1. Position of Serbia in Europe (left), position of Novi Sad in Serbia (center), and Vojvodina (right)

Source: https://sco.m.wikipedia.org/wiki/File:Novi_Sad_in_Serbia_and_Europe.png

Extreme precipitation events (EXPEs) were analyzed based on daily precipitation from 1961 to 2020 in Novi Sad, Serbia. The data used in this work includes daily precipitation amounts recorded at the station of Novi Sad (45°20' N; 19°51' E; 84 m altitude)

and is provided by the Serbian Meteorological Service, which technically and critically controlled these measurements.

Monthly values of Northern Hemisphere teleconnection patterns (North Atlantic Oscillation - NAO, Eastern Atlantic - EA, and Eastern Atlantic Western Russia - EAWR pattern) were downloaded from the Columbia Climate School (International Research Institute for Climate and Society) https://iridl.ldeo.columbia.edu/SOURCES/.Indices/.CPC_Indices/.NHTI/ for the period 1961–2020.

Methods

Climate indices

The Expert Team on Climate Change Detection and Indices (ETCCDI) has developed a set of 27 indices based on daily temperature and precipitation that are commonly used in climate change analysis (Alexander & Arblaster, 2017; Yin & Sun, 2018; Cooley & Chang, 2021). From this list, 9 indices are selected and presented in Table 1. The temporal characteristics of the following EXPEs were investigated: R10mm (Heavy precipitation days), R20mm (Very heavy precipitation days), Rx1day (Highest 1-day precipitation amount), Rx3day (Highest 3-day precipitation amount), Rx5day (Highest 5-day precipitation amount), R95p (Very wet days), R99p (Extremely wet days), R95pTot (Precipitation fraction due to very wet days) and R99pTot (Precipitation fraction due to extremely wet days). The EXPEs were analyzed on an annual and seasonal basis and for two reference periods 1961-1990 and 1991-2020.

The modified Man-Kendall (MMK) test

In this work we use the Mann-Kendall test modified by effective sample size to detect trends in serially correlated hydrological series, proposed by Yue and Wang (2004). The description of this MMK procedure is presented in (Stosic et al., 2024), and all the calculations are performed using open-source software (Patakamuri & O'Brien, 2021; R Core Team, 2023).

Table 1. Precipitation climate indices with their names, definitions and units

No	Index	Indicator name	Definitions	Unit
1	R10mm	Heavy precipitation days	Number of days where RR (daily precipitation) ≥ 10 mm	days
2	R20mm	Very heavy precipitation days	Number of days where RR ≥ 20 mm	days
3	RX1day	Highest 1-day precipitation amount	The maximum 1-day values for period j	mm
4	RX3day	Highest 3-day precipitation amount	The maximum 3-day values for period j	mm
5	RX5day	Highest 5-day precipitation amount	The maximum 5-day values for period j	mm
6	R95p	Very wet days	Number of days where RR (RR ≥ 1) ≥ 95 th percentile	days
7	R99p	Extremely wet days	Number of days where RR (RR ≥ 1) ≥ 99 th percentile	days
8	R95pTot	Precipitation fraction due to very wet days	$R95pTot_j = 100 \frac{\sum RR_{wj}}{RR_j}$, where $RR_{wj} > RR_{wn}95$	%

9	R99pTot	Precipitation fraction due to extremely wet days	$R99pTot_j = 100 \frac{\sum RR_{wj}}{RR_j}$, where $RR_{wj} > RR_{wn}99$	%
---	---------	--	--	---

The large-scale teleconnection patterns (LSTP)

The following teleconnection patterns, the North Atlantic Oscillation (NAO), East Atlantic pattern (EA) and East Atlantic Western Russia (EAWR) pattern are considered to investigate possible influence of the LSTP on EXPEs. The NAO consists of two centers of action being located near Iceland and the Azores and has a positive correlation with precipitation in Northern and Western Europe, and a negative one over Southern Europe, including Serbia (Hurrell, 1995). The EA pattern is characterized by two anomaly centers that are displaced southeastward to the approximate nodal lines of the NAO pattern (Barnston & Livezey, 1987). According to Krichak et al. (2014), the EAWR pattern is associated with negative geopotential height anomalies over the North Atlantic and the area north of the Caspian Sea and positive geopotential height anomalies over Western Europe and Northern China. Tošić and Putniković (2021) pointed out that precipitation over Serbia is negatively correlated with the EAWR. To examine links between EXPEs and LSTP, the Pearson correlation was used and calculated using the open-source software tool “Scipy”, Python library. The Student’s *t*-test at the 0.05 significance level was applied to check the significance of correlation.

Results

Seasonal analysis

Heavy precipitation days (R10mm)

Figure 2 shows the seasonal values of heavy precipitation days (R10mm). Looking at all seasons, the highest number of days with more than or equal to 10 mm is recorded in summer. The mean value of R10mm is highest in summer in both periods: 6.3 from 1961 to 1990 and 7.6 from 1991 to 2020 (Table 2). However, the highest R10mm value (21) is observed in spring in the period 1991-2020 (Table 2). All seasonal values increased in the second period, except for the minimum value of R10mm in fall, which was 0 in 2018. The maximum value of R10mm was measured in the spring (21) and summer (19) of 2014 at the Novi Sad station.

Table 2. Minimum, mean and maximum values of R10mm during two periods: 1961-1990 and 1991-2020

R10mm	1961 - 1990			1991 - 2020			
	season	min	mean	max	min	mean	max
Winter	Winter	0	3.1	10	0	3.7	10
Spring	Spring	0	4	10	0	5.7	21
Summer	Summer	1	6.3	16	2	7.6	19
Fall	Fall	1	4.0	10	0	6.2	13

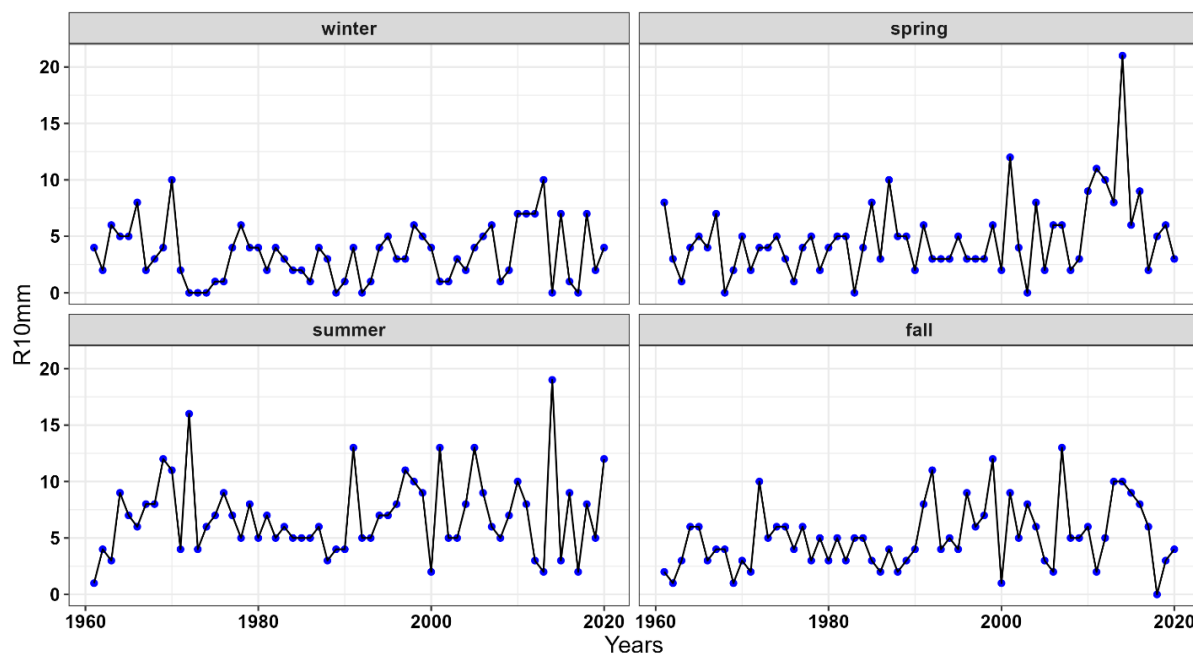


Figure 2. Seasonal values of R10mm during the period 1961-2020 in Novi Sad

Very heavy precipitation days (R20mm)

The seasonal values of very heavy precipitation days (R20mm) are shown in Fig. 3. There was a low number of R20mm in all seasons except summer (Fig. 3). The lowest number of heavy precipitation days was recorded in winter. The mean value of R20mm was 0.4 from 1961 to 1990 and 0.5 from 1991 to 2020 (Table 3). On the other hand, the mean value of R20mm was 2.4 from 1961 to 1990 and 3.2 during the second period in summer, with a maximum value of 9 and 8.

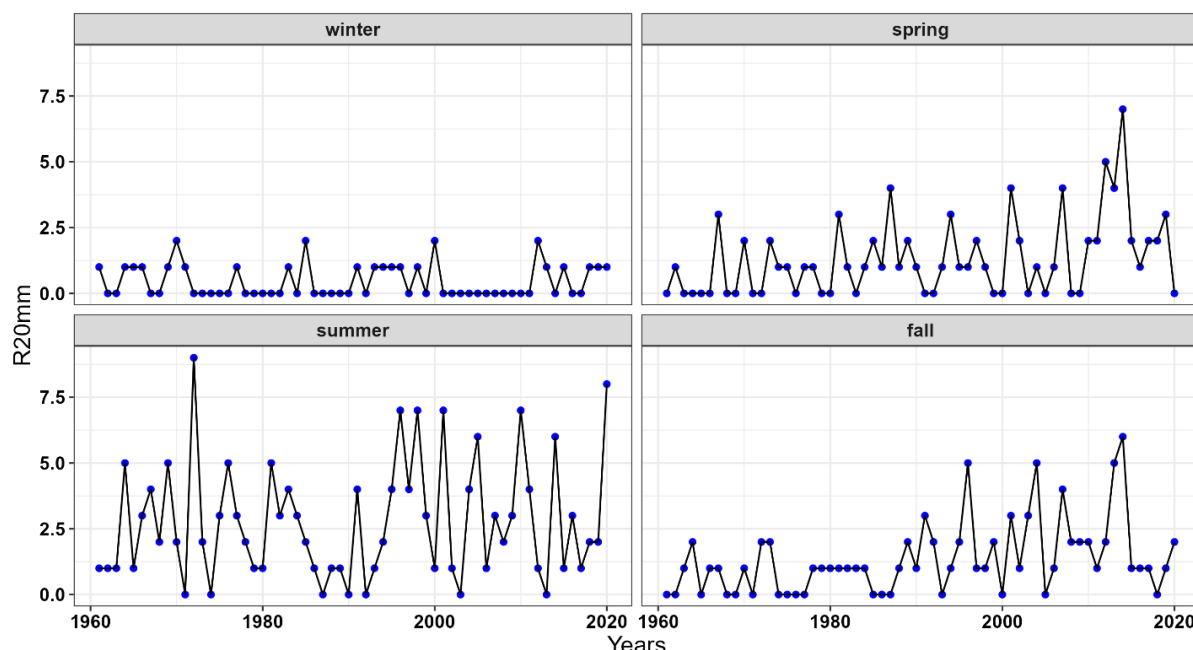


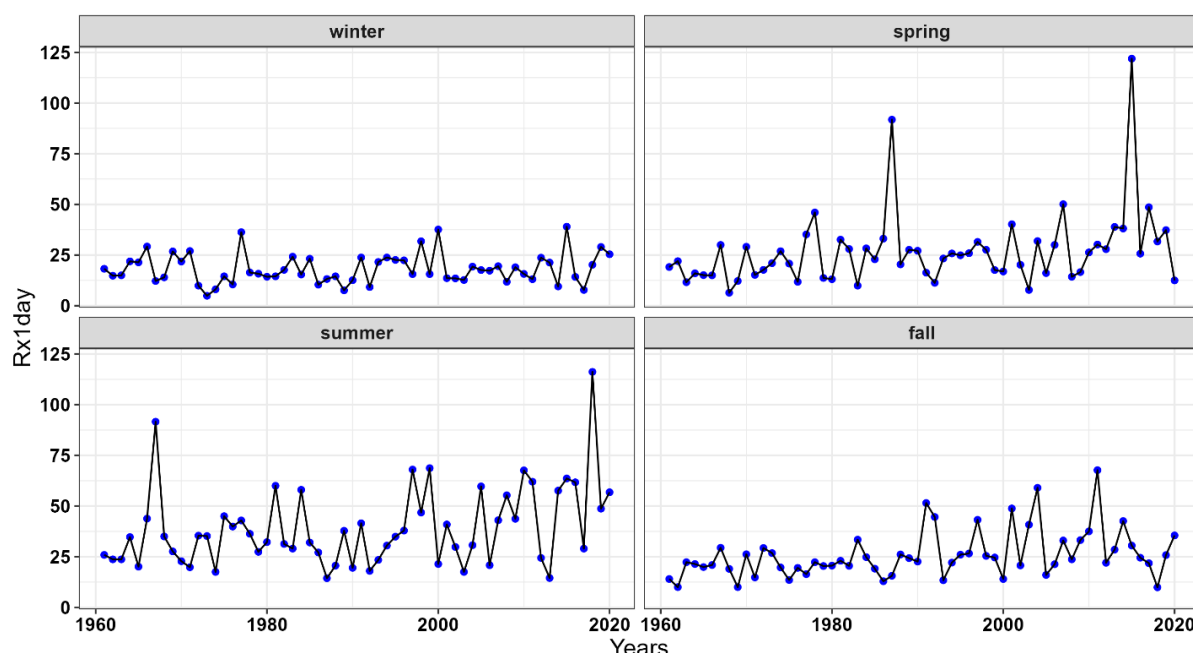
Figure 3. Seasonal values of R20mm during the period 1961-2020 in Novi Sad

Table 3. Minimum, mean and maximum values of R20mm during two periods: 1961-1990 and 1991-2020

R20mm	1961 - 1990			1991 - 2020			
	season	min	mean	max	min	mean	max
Winter		0	0.4	2	0	0.5	2
Spring		0	0.9	4	0	1.7	7
Summer		0	2.4	9	0	3.2	8
Fall		0	0.7	2	0	2	6

Highest 1-day precipitation amount (Rx1day)

Figure 4 shows the seasonal values of the highest 1-day precipitation amount (Rx1day). Daily precipitation was below 40 mm in winter and below 70 mm in fall (Fig. 4). There were two peaks for Rx1day in spring, 121.9 mm in 2015 and 91.8 mm in 1987. The highest 1-day precipitation values were measured in summer (Fig. 4). The mean values of Rx1day were highest during the summer season in both periods considered, 33.7 in the first and 44.5 in the second period (Table 4). All descriptive statistics increased in the second period 1991-2020, except for the mean and peak in winter (Table 4).

**Figure 4.** Seasonal values of Rx1day during the period 1961-2020 in Novi Sad**Table 4.** Minimum, mean and maximum values of Rx1day during two periods: 1961-1990 and 1991-2020

Rx1day	1961 - 1990			1991 - 2020			
	season	min	mean	max	min	mean	max
Winter		4.9	16.9	36.3	7.0	7.8	19.6
Spring		6.4	24.0	91.8	7.8	29.6	121.9
Summer		14.4	33.7	91.6	14.5	44.5	116.2
Fall		10	20.6	33.4	9.9	31.1	67.7

Highest 3-day precipitation amount (Rx3day) and Highest 5-day precipitation amount (Rx5day)

Rx3day and Rx5day are shown in Fig. 5 and Fig. 6 respectively. As in the case of Rx1day, the lowest values of both indices were recorded in winter. Higher values of Rx3day (Fig. 5) and Rx5day (Fig. 6) are recorded in the fall than in the winter. Two maxima can be observed in spring: 149.4 mm in 2015 and 102.6 mm in 1987 for Rx3day (Table 5) and 162.3 mm in 2015 and 104.7 mm in 1987 for Rx5day (Table 6). The minimum, mean and maximum values of both indices increased from 1991 to 2020 compared to 1961-1990, with the exception of the minimum values of Rx3day (Table 5) and Rx5day (Table 6) during the fall season.

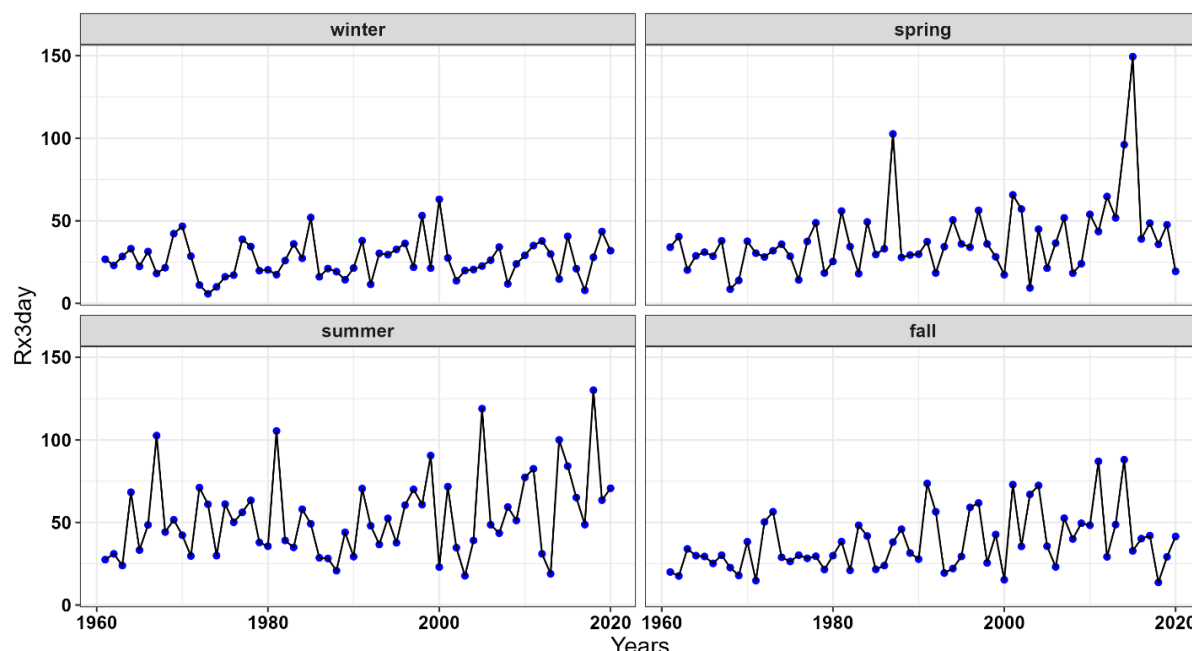


Figure 5. Seasonal values of Rx3day during the period 1961-2020 in Novi Sad

Table 5. Minimum, mean and maximum values of Rx3day during two periods: 1961-1990 and 1991-2020

Rx3day	1961 - 1990			1991 - 2020		
season	min	mean	max	min	mean	max
Winter	5.8	24.9	52	7.9	28.6	63
Spring	8.6	33.0	102.6	9.4	44.2	149.4
Summer	20.8	46.9	105.4	17.7	60.2	130.1
Fall	14.8	30.6	56.5	13.7	45.2	88

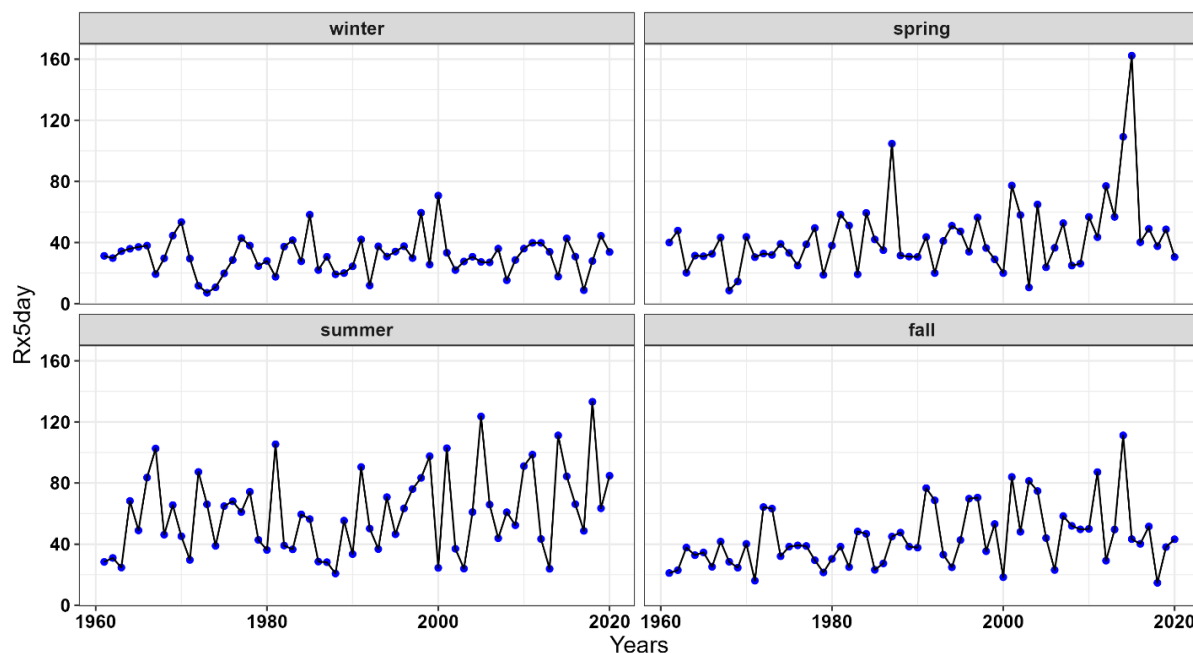


Figure 6. Seasonal values of Rx5day during the period 1961-2020 in Novi Sad

Table 6. Minimum, mean and maximum values of Rx5day during two periods: 1961-1990 and 1991-2020

Rx5day	1961 - 1990			1991 - 2020		
	min	mean	max	min	mean	max
Winter	7.1	29.8	58.2	8.8	32.8	70.7
Spring	8.6	37.1	104.7	10.6	48.8	162.3
Summer	20.8	52.6	105.4	23.9	68.7	133.2
Fall	16.1	35.4	64.3	14.7	52.2	111.2

Very wet days (R95p)

Very wet days are shown in Fig. 7. The values of R95p were lower than 13 days in all seasons. The only exception was spring 2014, when 19 days were observed in Novi Sad. The descriptive statistics (mean and maximum values) presented in Table 7 show that all seasonal values increased in the period 1991-2020. The highest increase in the maximum value of R95p is observed in the spring, from 9 to 19 in the second period (Table 7).

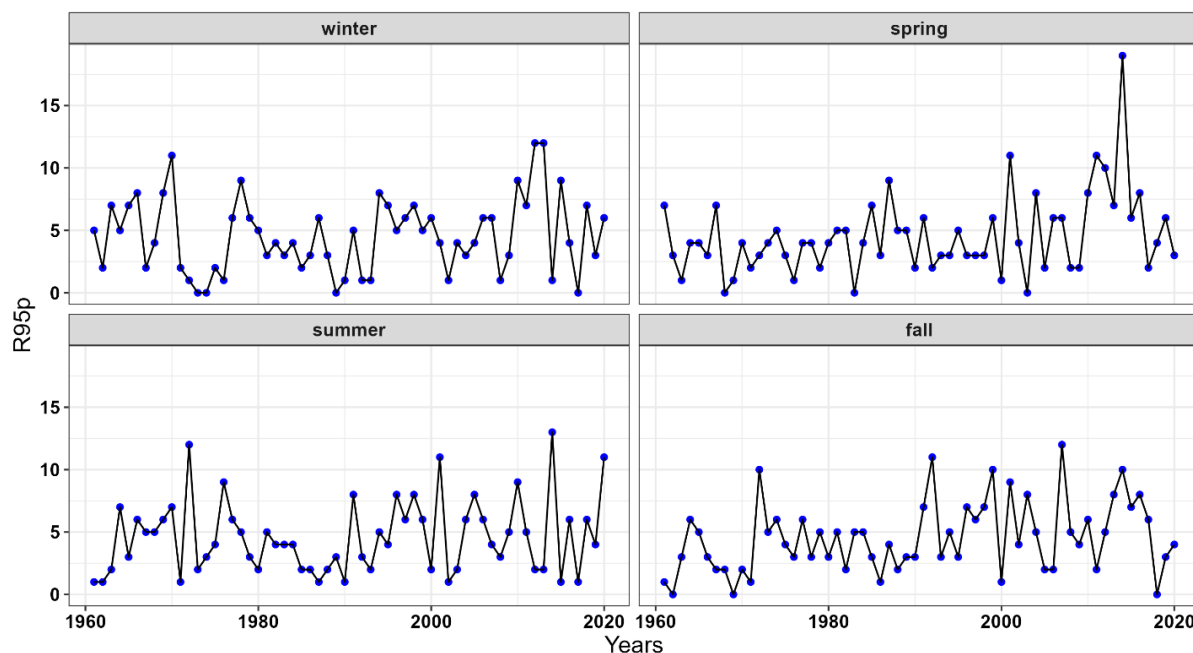


Figure 7. Seasonal values of R95p during the period 1961-2020 in Novi Sad

Table 7. Minimum, mean and maximum values of R95p during two periods: 1961-1990 and 1991-2020

R95p	1961 - 1990			1991 - 2020		
season	min	mean	max	min	mean	max
Winter	0	4	11	0	5.1	12
Spring	0	3.7	9	0	5.3	19
Summer	1	3.9	12	1	5.3	13
Fall	0	3.4	10	0	5.7	12

Extremely wet days (R99p)

The extremely wet days are shown in Fig. 8. In general, the number of days greater than or equal to the 99th percentile was low (less than 3) in all seasons. Five days with R99p were observed in winter (2013) and spring (2014), 7 in summer (2010) and six in fall (2014). Table 8 shows that the mean and maximum values of R99p increased in all seasons. The minimum number of R99p values was zero in the period 1961-2020.

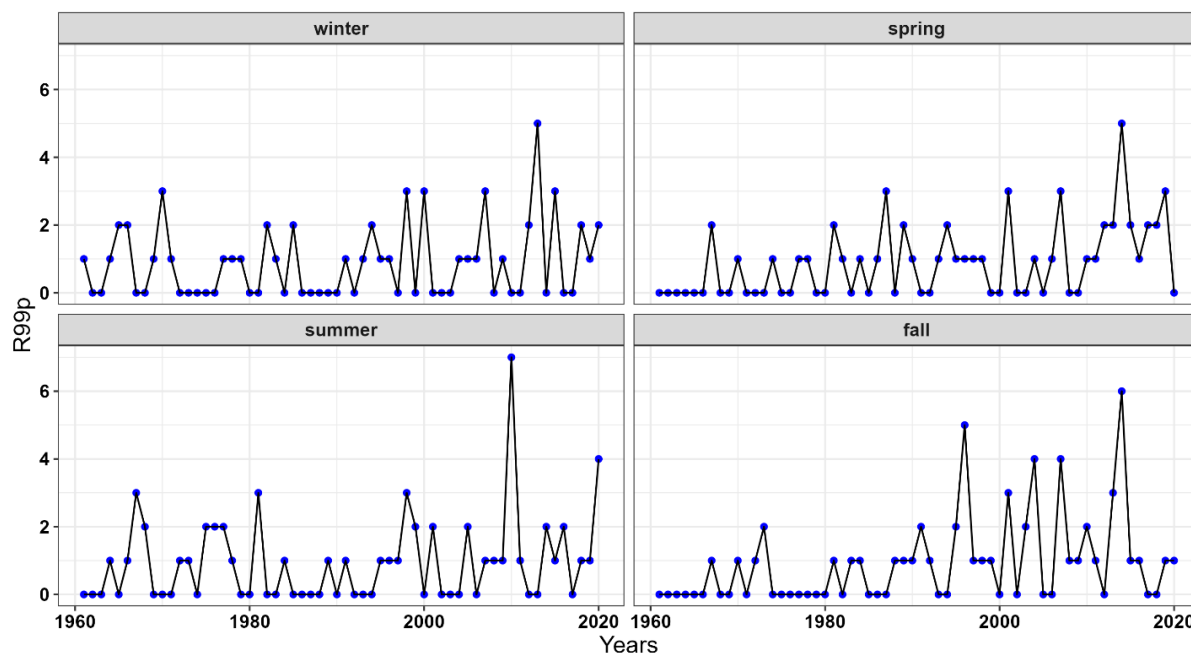


Figure 8. Seasonal values of R99p during the period 1961-2020 in Novi Sad

Table 8. Minimum, mean and maximum values of R99p during two periods: 1961-1990 and 1991-2020

R99p	1961 - 1990			1991 - 2020		
season	min	mean	max	min	mean	max
Winter	0	0.6	3	0	1.1	5
Spring	0	0.6	3	0	1.2	5
Summer	0	0.7	3	0	1.2	7
Fall	0	0.4	2	0	1.5	6

Precipitation fraction due to very wet days (R95pTot)

The seasonal values of precipitation fraction due to very wet days (R95pTot) are shown in Fig. 9. The values of R95pTot increase in all seasons (Fig. 9), as can be seen for the mean and maximum values of R95pTot in Table 9. The highest increase in the mean and maximum values of R95pTot is observed in the fall (Table 9).

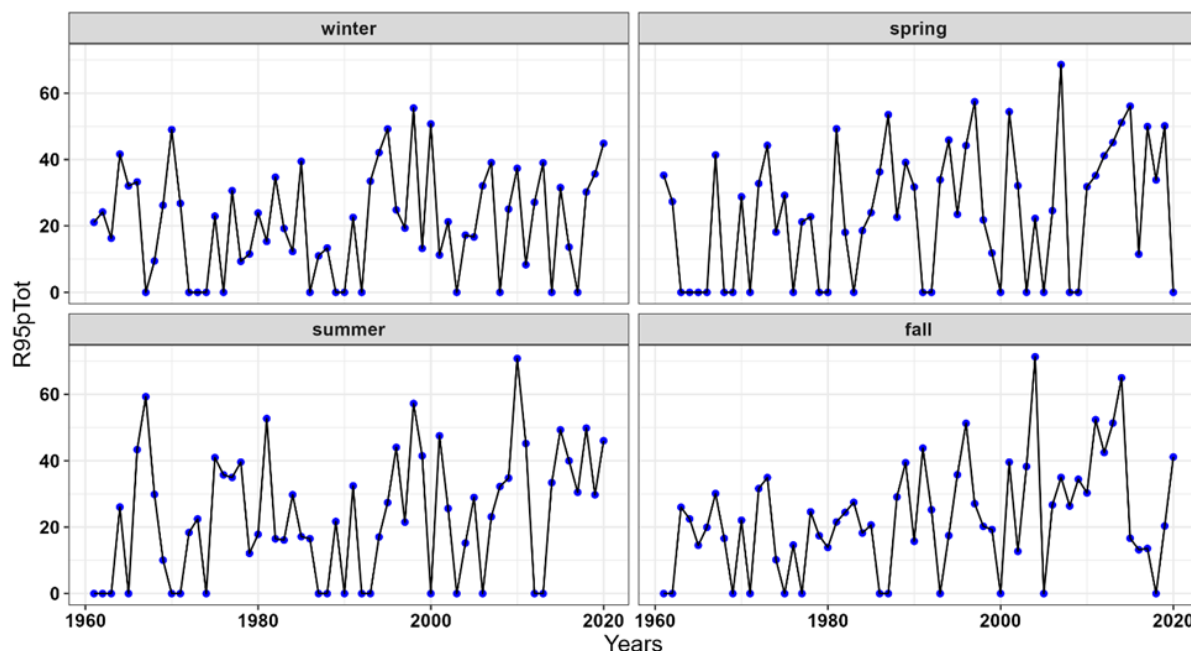


Figure 9. Seasonal values of R95pTot during the period 1961-2020 in Novi Sad

Table 9. Minimum, mean and maximum values of R95pTot during two periods: 1961-1990 and 1991-2020

R95pTot	1961 - 1990			1991 - 2020		
	min	mean	max	min	mean	max
Winter	0	17.4	49.0	0	24.7	55.5
Spring	0	19.8	53.5	0	28.2	68.6
Summer	0	18.7	59.3	0	28.1	70.8
Fall	0	16.5	39.4	0	29.0	71.3

Precipitation fraction due to extremely wet days (R99pTot)

Precipitation fraction due to extremely wet days (R99pTot) is shown in Fig. 10. Although it appears that the percentage of R99pTot is higher in winter in the first period (Fig. 10), Table 10 shows that the mean value of R99pTot is higher in the second period (7.9) than in the first period (5.5). This was a consequence of the high R99pTot values from 1991 to 2000 (Fig. 10). It can be seen that the percentage of precipitation attributable to extremely wet days was greater in spring, summer and fall in the second period (Fig. 10). The mean and maximum values of R99pTot increased in the second period, with the highest increase occurring in the fall (Table 10). For example, the mean value of R99pTot increased from 0.9 in the period 1961-1990 to 11.7 in the period 1991-2020, while the maximum value of R99pTot doubled (from 27.5 to 54.0).

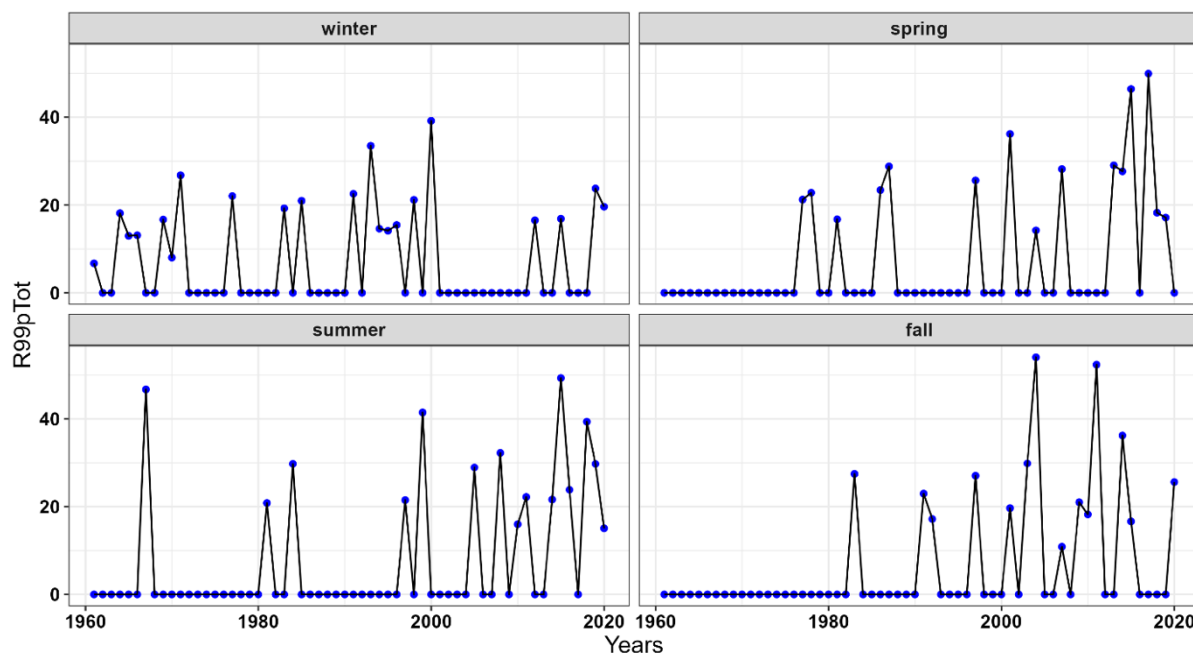


Figure 10. Seasonal values of R99pTot during the period 1961-2020 in Novi Sad

Table 10. Minimum, mean and maximum values of R99pTot during two periods: 1961-1990 and 1991-2020

R99pTot	1961 - 1990			1991 - 2020		
season	min	mean	max	min	mean	max
Winter	0	5.5	26.8	0	7.9	39.2
Spring	0	3.8	28.8	0	9.8	49.9
Summer	0	3.2	46.7	0	11.4	49.3
Fall	0	0.9	27.5	0	11.7	54.0

Trend analysis of seasonal EXPEs

The trend of EXPEs was calculated for all seasons and results obtained using the MMK test were presented in Table 11 for winter, Table 12 for spring, Table 13 for summer and Table 14 for fall. Table 11 shows that a positive trend prevailed in winter. A negative trend was identified for R20mm and R99pTot in winter (Table 11). There was no significant trend for seven indices. A significant positive trend was only observed for R95pTot and Rx3days. A significant positive trend was observed for all indices in spring (Table 12) and fall (Table 14). A significant positive trend was observed for R95pTot, R99pTot, Rx1day, Rx3day and Rx5day in summer (Table 13).

Table 11. The Modified Mann- Kendall test results (Z), p-value (pv), Sen's slope (sen) and trend (trend_mdf) for time series of all indices in winter

Index	Z	pv	sen	trend_mdf
R10mm	0.8640	0.3875	0	No Trend
R20mm	-0.1215	0.9032	0	No Trend
R95p	1.1622	0.2451	0	No Trend
R95pTot	2.1818	0.0291	0.0620	Positive Trend
R99p	1.4151	0.1570	0	No Trend
R99pTot	-0.9462	0.3440	0	No Trend
Rx1day	1.6098	0.1074	0.0333	No Trend
Rx3day	3.0160	0.0025	0.0833	Positive Trend
Rx5day	1.0458	0.2956	0.0290	No Trend

Table 12. The Modified Mann- Kendall test results (Z), p-value (pv), Sen's slope (sen) and trend (trend_mdf) for time series of all indices in spring

Index	Z	pv	sen	trend_mdf
R10mm	3.0790	0.0020	0.0384	Positive Trend
R20mm	4.5340	5.78E-06	0.0198	Positive Trend
R95p	4.0652	4.79E-05	0.0454	Positive Trend
R95pTot	7.3259	2.37E-13	0.2818	Positive Trend
R99p	2.3198	0.0203	0	Positive Trend
R99pTot	2.1617	0.0306	0	Positive Trend
Rx1day	6.5839	4.58E-11	0.2426	Positive Trend
Rx3day	4.7071	2.51E-06	0.3010	Positive Trend
Rx5day	4.1435	3.42E-05	0.3064	Positive Trend

Table 13. The Modified Mann- Kendall test results (Z), p-value (pv), Sen's slope (sen) and trend (trend_mdf) for time series of all indices in summer

Index	Z	pv	sen	trend_mdf
R10mm	1.2335	0.2173	0	No Trend
R20mm	1.3318	0.1829	0	No Trend
R95p	1.4315	0.1522	0	No Trend
R95pTot	5.7474	9.067E-09	0.3224	Positive Trend
R99p	1.8878	0.0590	0	No Trend
R99pTot	2.4546	0.0141	0	Positive Trend
Rx1day	4.8792	1.06E-06	0.35	Positive Trend
Rx3day	5.0675	4.03E-07	0.3827	Positive Trend
Rx5day	4.4239	9.69E-06	0.3802	Positive Trend

Table 14. The Modified Mann- Kendall test results (Z), p-value (pv), Sen's slope (sen) and trend (trend_mdf) for time series of all indices in fall

Index	Z	pv	sen	trend_mdf
R10mm	5.5435	2.96E-08	0.0434	Positive Trend
R20mm	4.1394	3.48E-05	0.0200	Positive Trend
R95p	7.1969	6.15E-13	0.0510	Positive Trend
R95pTot	8.2301	1.86E-16	0.3374	Positive Trend
R99p	2.2884	0.0221	0	Positive Trend
R99pTot	2.2294	0.0257	0	Positive Trend
Rx1day	5.7814	7.40E-09	0.2000	Positive Trend
Rx3day	6.3697	1.89E-10	0.3211	Positive Trend
Rx5day	6.3408	2.28E-10	0.3546	Positive Trend

Annual analysis

The annual analysis shows an increase in all indices (Fig. 11 and Table 15). The number of days with more than 10 mm (R10mm) and 20 mm (R20mm) was highest in 2014, 53 and 20, respectively (Fig. 11). The highest daily precipitation (Rx1day) was 121.9 mm in 2015 (Fig. 11). In addition, the highest 3-day (Rx3day) and 5-day precipitation amounts (Rx5day) were measured in 2015, 149.4 and 162.3 mm, respectively. The secondary maximum was observed in 2018, 116.2 mm for Rx1day, 130.1 mm for Rx3day and 133.2 mm for Rx5day. The highest number of very wet days (R95p) and extremely wet days (R99p) was 51 and 16 respectively in 2014 (Fig. 11). As can be seen from Fig. 11, significantly more R95Tot and R99Tot occurred after 1995. In Novi Sad, a significant positive trend was observed for all indices (Table 15).

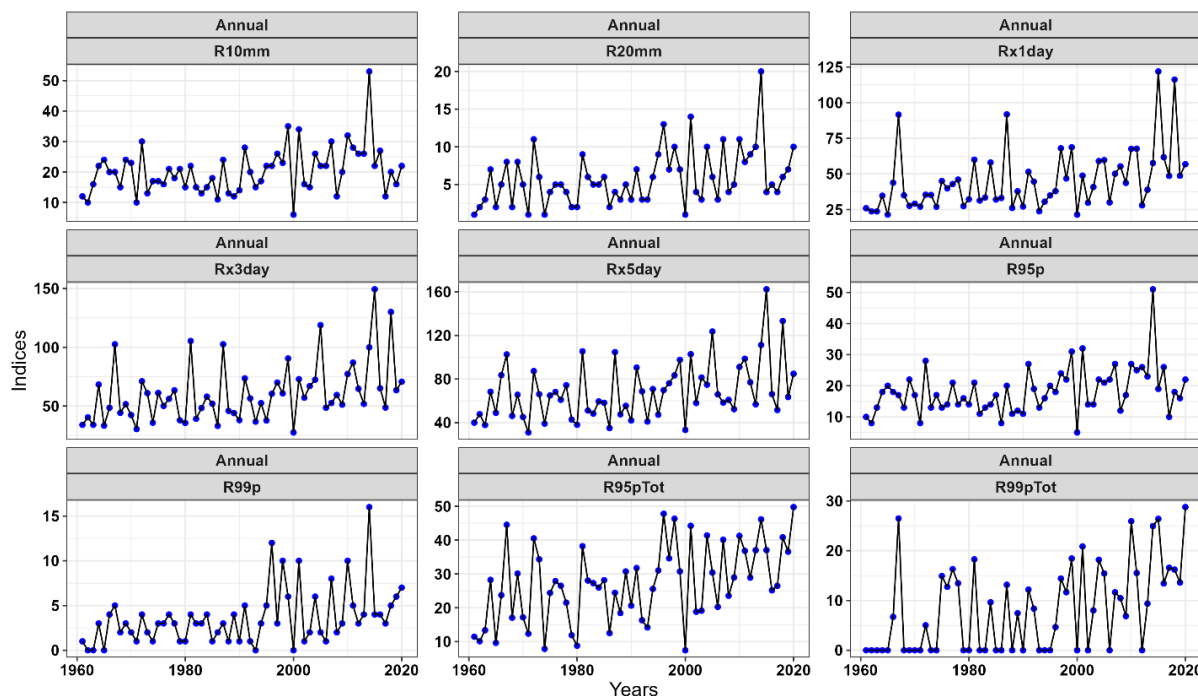


Figure 11. Annual values of climate indices listed in Table 1 during the period 1961-2020 in Novi Sad

Table 15. The Modified Mann- Kendall test results (Z), p-value (pv), Sen's slope (sen) and trend (trend_mdf) for the annual time series of all indices during the period 1961-2020

Index	Z	pv	Sen	trend_mdf
R10mm	5.1871	2.14E-07	0.1234	Positive Trend
R20mm	8.6622	4.63E-18	0.0714	Positive Trend
R95p	6.9202	4.51E-12	0.1428	Positive Trend
R95pTot	11.370	5.9E-30	0.3261	Positive Trend
R99p	6.5170	7.17E-11	0.0555	Positive Trend
R99pTot	7.7639	8.23E-15	0.2186	Positive Trend
Rx1day	9.1368	6.43E-20	0.4586	Positive Trend
Rx3day	8.0207	1.05E-15	0.4898	Positive Trend
Rx5day	7.3926	1.44E-13	0.5131	Positive Trend

The statistical analysis was then carried out for two reference periods 1961-1990 and 1991-2020. The results are shown in Table 16. The comparison of the values in the two periods under consideration shows that the mean and maximum values of all indices increased in the second period (Table 16). The minimum values of all indices fell or remained the same in the period 1991-2020, with the exception of Rx5day.

Table 16. Minimum, mean and maximum values of climate indices during two periods: 1961-1990 and 1991-2020

Index	1961 - 1990			1991 - 2020		
	min	mean	max	min	mean	max
R10mm	10.0	17.4	30.0	6.0	23.2	53.0
R20mm	1.0	4.4	11.0	1.0	7.3	20.0
Rx1day	21.4	38.2	91.8	21.4	51.9	121.9
Rx3day	30.4	52.3	105.4	27.5	69.2	149.4
Rx5day	31.0	58.9	105.4	33.3	78.4	162.3
R95p	8.0	15.1	28.0	5.0	21.3	51.0
R99p	0	2.3	5.0	0	4.9	16.0
R95pTot	7.9	22.5	44.5	7.4	31.9	49.8
R99pTot	0	4.8	26.5	0	11.7	28.8

An influence of the large-scale circulation on extreme precipitation events (EXPEs)

In order to investigate the influence of the large-scale atmospheric circulation on the EXPEs in Novi Sad, the Pearson correlation coefficient was calculated, the results of which are shown in Table 17. A positive correlation was found between the climate indices and the EA pattern and a negative correlation with the EAWR pattern (Table 17). A significant positive correlation was found between R95p, R95pTot, R99p, R99pTot, Rx1day, Rx3day, Rx5day and EA, and a strong negative correlation between R20mm, R95p, R95pTot, R99p, R99pTot and EAWR. The influence of NAO on EXPEs was weak during the whole 1961-2020 period in Novi Sad.

Table 17. Correlation coefficient between the climate indices listed in Table 1 and teleconnection patterns: the North Atlantic Oscillation (NAO), the East Atlantic pattern (EA) and the East Atlantic Western Russia (EAWR) pattern

Index	NAO	EA	EAWR
R10mm	-0.0808	0.2259	-0.2249
R20mm	-0.0392	0.2239	-0.3245
R95p	-0.0762	0.2617	-0.2591
R95pTot	0.0854	0.2997	-0.3133
R99p	-0.0544	0.3087	-0.3857
R99pTot	0.0774	0.3311	-0.3984
Rx1day	0.2173	0.3280	-0.2527
Rx3day	0.1668	0.3165	-0.2519
Rx5day	0.1495	0.3085	-0.2223

Coefficients being significant at the 5% level are bolded

Discussion

The EXPEs were examined on an annual and seasonal basis and for two reference periods (1961-1990 and 1991-2020). We investigated the following indices: R10mm, R20mm, Rx1day, Rx3day, Rx5day, R95p, R99p, R95pTot and R99pTot. The Modified Mann–Kendall (MMK) test was used to assess trends in the EXPEs series over two time periods considered. Compared to the classical Mann–Kendall (MK) test, the MMK offers the advantage of reducing bias from serial dependence in time series while retaining the robustness and non-parametric, distribution-free properties of the original MK test. In our study, positive trends were observed for all annual and seasonal values of the indices with the exception of R20mm and R99pTot in winter. A significant positive trend was obtained for all annual values, spring and fall seasons. Leščešen et al. (2023) applied the peak-over-threshold method for the same 1961-2020 period as we did, with the threshold set at the 90th percentile, and found a significant increase in the frequency of extreme precipitation. For example, a total of 11 extreme years occurred from 2000 onwards, compared to six events before 2000 (Leščešen et al., 2023). Savić et al. (2020) analyzed the possible influence of urban factors on EXPEs in Novi Sad by establishing precipitation-climate indices and proposing to relate them to the pluvial flood hazard according to historical events.

In 2014, extreme rainfall of more than 200 mm in 72 hours was recorded and catastrophic flooding occurred in Bosnia, Croatia and Serbia (Tošić et al., 2014). An area of around 20,000 km² was flooded, which was unprecedented (Tošić et al., 2017). The maximum annual values of RR10mm, RR20mm, Rx1day, Rx3day, Rx5day, R95p and R99p were also measured in Novi Sad in 2014 (Fig. 11). A significant increase in Rx1day, Rx3day and Rx5day was observed in all seasons (with the exception of Rx1day and Rx5day in winter) and on an annual basis. High mean values of Rx1day (39.1 mm), Rx3day (53.6 mm) and Rx5day (60.6 mm) were measured in summer (Figs. 4, 5 and 6), compared to other seasons. The mean values of Rx1day, Rx3day and Rx5day were 25.9 mm, 37.9 mm and 43.8 mm in fall, 26.8 mm, 38.6 mm and 42.9 mm in spring, while lower values of 18.2 mm, 26.7 mm and 31.3 mm were recorded in winter, respectively. The high summer value of Rx1day (116.6 mm) was measured in Novi Sad in 2018, caused by convective rainfall, which led to flooding in the city due to a high proportion of impermeable surfaces and limited drainage systems (Savić et al., 2020). The meteorological situation that led to this flooding episode is shown in Fig. 12a. Figure 12a shows that Serbia is located in a region with increased geopotential and is under the influence of a very warm air mass. A low-pressure area is located much further north. A vertical profile

of the temperature over Belgrade (sounding station closest to Novi Sad) on June 29, 2018 using data from the University of Wyoming (<https://weather.uwyo.edu/upperair/sounding.html>) and applying the Metpy Python library (May et al., 2022) is shown in Fig. 12b. The negative Lifted Index (-3.20), the high CAPE value (1093.93 J/kg) and the favorable K (36) and Totals Totals (TT) indices (47.6) indicate an environment that favors strong convective development and leads to severe thunderstorms. A high temperature and a very unstable atmosphere favored strong convection and caused the heaviest precipitation in northern Serbia. Precipitation was locally very intense (Fig. 13), which is confirmed by the fact that the value of RX1day for Novi Sad on June 29, 2018 was 116.6 mm, which is three times the average summer RX1day (39.1 mm). Our results are in line with the findings of other researchers (Marchi et al., 2010; Guerreiro et al., 2017), who found that flash floods in continental climates occur more frequently in the spring or summer months.

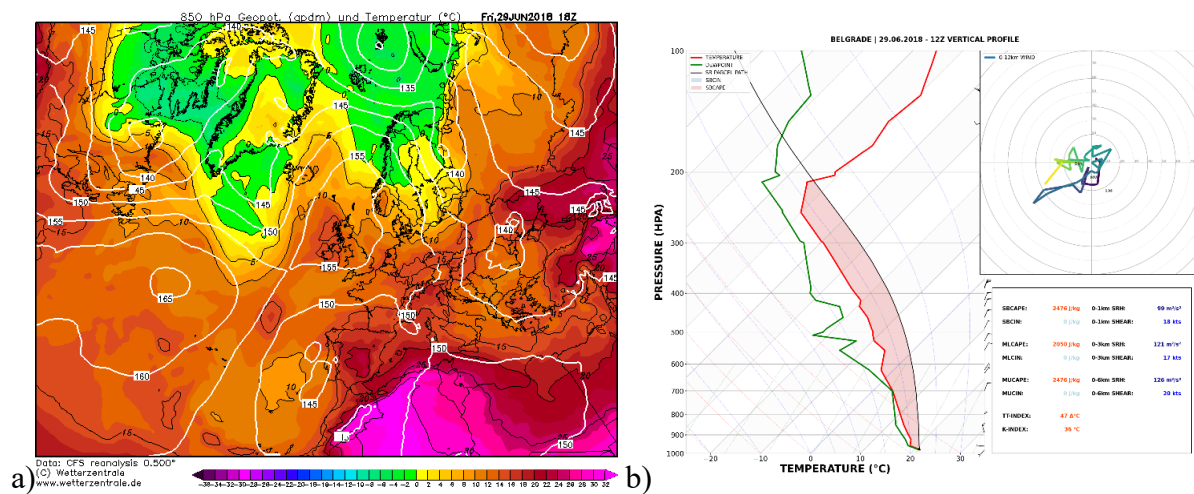


Figure 12. (a) 850 hPa Geopotential Height obtained from reanalysis (wetterzentrale.de) and (b) vertical profile for Belgrade for 29/06/2018 at 18 UTC

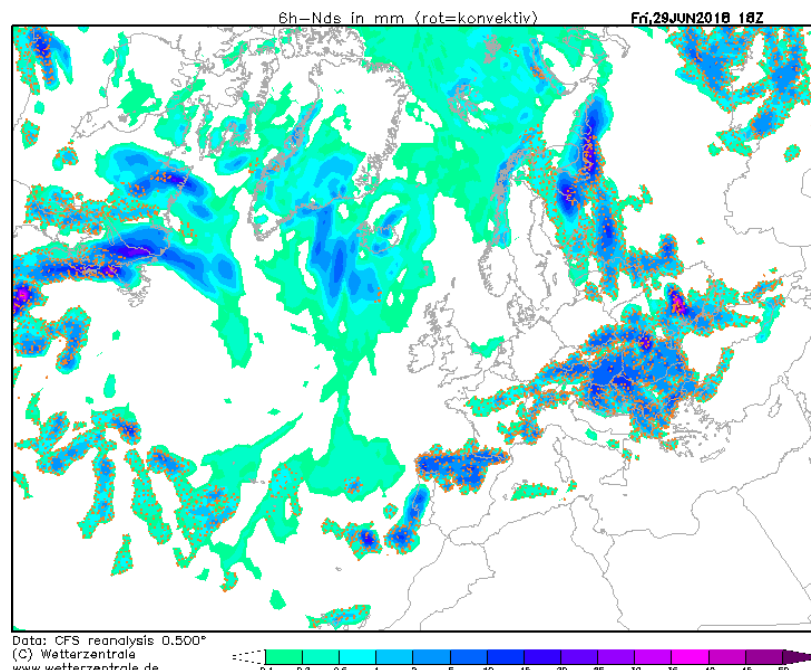


Figure 13. Precipitation data for 29/06/2018 at 18 UTC obtained from reanalysis (wetterzentrale.de)

This research and its results can contribute to the local community by providing reliable indicators of the increasing frequency and intensity of extreme precipitation, which is crucial for planning adaptation measures and reducing flood risk. The data obtained can be used to establish early warning systems, to adapt infrastructure - including the construction of more resilient buildings and the improvement of drainage systems (Yang et al., 2020; Mehvar et al. 2021) - and to support responsible spatial planning, thereby strengthening the resilience of the local population. In addition, the data can be useful for planning and investing in flood defence infrastructure (protective walls, dikes) as well as green infrastructure, a comprehensive approach that incorporates natural elements such as wetlands, green roofs and permeable pavements into urban planning (Dharmarathne et al., 2024). In this way, research contributes directly to the protection of public health (Sustainable Development Goals - SDG 3), the development of sustainable and safe cities and settlements (SDG 11) and the implementation of climate action through adaptation to change (SDG 13).

It should be emphasized that a strong positive correlation was found between the annual values of the climate indices R95p, R95Tot, R99p, R99pTot, Rx1day, Rx3day and Rx5day and EA, and a negative correlation between RR20mm, R95p, R95Tot, R99p, R99pTot and EAWR pattern. A correlation between the indices and the NAO was weak (Table 17). This result was not expected, as previous literature found a strong influence of the NAO on precipitation in Serbia (Tošić, 2004) and Vojvodina (Tošić et al., 2014). In their studies (Tošić, 2004; Tošić et al., 2014), the annual precipitation totals were analyzed, while in our case the number of days with daily precipitation greater than or equal to 10 mm, 20 mm and the 95th and 99th percentiles, as well as the fraction of precipitation due to very wet and extremely wet days were investigated. A negative correlation between EXPEs and the EAWR was expected, as Tošić and Putniković (2021) indicated that there was a precipitation surplus in Serbia when the EAWR was in a negative phase. A strong positive influence of the EA pattern on the temperature-climate indices in Serbia, including Novi Sad, was also found by Tošić et al. (2023). According to Ruml et al. (2017), the positive phase of the EA is associated with the transport of warm air over Serbia. In a warming climate, more frequent extreme precipitation events are expected.

Conclusions

Extreme precipitation events (EXPEs) were analyzed on the basis of daily precipitation recorded in Novi Sad, Serbia. The absolute and percentile climate indices were analyzed on an annual and seasonal basis for the entire observation period 1961-2020 and for two reference periods (1961-1990 and 1991-2020). All indices increased in the period 1991-2020 compared to the period 1961-1990, with the exception of R20mm and R99pTot in winter. A significant increase in Rx1day, Rx3day and Rx5day was observed in all seasons (except Rx1day and Rx5day in winter) and on an annual basis. This indicates an increasing frequency of high intensity precipitation events, especially in spring and summer. Of all the indices considered, Rx1day was found to be most strongly related to flood risk. The high value of Rx1day (116.6 mm) was measured in Novi Sad in the summer of 2018, when flooding occurred in Novi Sad. The intense rainfall was of convective origin and led to flooding in the city due to local terrain characteristics and limited drainage systems. The possible influence of large-scale circulation patterns on EXPEs was investigated. A significant positive correlation was found between R95p, R95pTot, R99p, R99pTot, Rx1day, Rx3day and Rx5day and EA, and a strong negative correlation between R20mm, R95p, R95Tot, R99p, and R99pTot and EAWR. Since a significant positive trend was observed for all annual

EXPEs, it is to be expected that extreme daily precipitation will occur more frequently in the future. It is therefore necessary to prepare for heavy precipitation, which can lead to flooding.

Acknowledgments

The authors would like to thank the Hydrometeorological Service of Serbia, which provided the data necessary for this study. I.T., L.F., S.P. and V.D. acknowledge support of the Ministry of Science, Technological Development and Innovation of the Republic of Serbia, grant No. 451-03-136/2025-03/200162. A.S.A.S., T.S and B.S acknowledge support of Brazilian agencies CAPES and CNPq (grants No 306590/2024-7, 308782/2022-4 and 309499/2022-4). This research was supported by the Science Fund of the Republic of Serbia, No. 7389, Project Extreme weather events in Serbia - analysis, modelling and impacts" – EXTREMES.

References

Alexander, L.V., & Arblaster, J.M. (2017). Historical and projected trends in temperature and precipitation extremes in Australia in observations and CMIP5. *Weather and Climate Extremes*, 15, 34–56. <https://doi.org/10.1016/j.wace.2017.02.001>

Bajat, B., Blagojević, D., Kilibarda, M., Luković, J., & Tošić, I. (2015). Spatial analysis of the temperature trends in Serbia during the period 1961–2010. *Theoretical and Applied Climatology*, 121, 289–301. <https://doi.org/10.1007/s00704-014-1243-7>

Barnston, A.G., & Livezey, R.E. (1987). Classification, seasonality and persistence of low-frequency atmospheric circulation patterns. *Monthly Weather Review*, 115, 1083–112. [https://doi.org/10.1175/1520-0493\(1987\)115<1083:CSAPOL>2.0.CO;2](https://doi.org/10.1175/1520-0493(1987)115<1083:CSAPOL>2.0.CO;2)

Berényi, A., Bartholy, J., & Pongrácz R. (2023). Analysis of precipitation-related climatic conditions in European plain regions. *Weather and Climate Extremes*, 42, 100610. <https://doi.org/10.1016/j.wace.2023.100610>

Bezdan, J., Bezdan, A., Blagojević, B., Antić, S., Greksa, A., Milić, D., & Lipovac, A. (2024). Impact of Climate Change on Extreme Rainfall Events and Pluvial Flooding Risk in the Vojvodina Region (North Serbia). *Atmosphere*, 15(4), 488. <https://doi.org/10.3390/atmos15040488>

Cooley, A.K., & Chang, H. (2021). Detecting change in precipitation indices using observed (1977–2016) and modeled future climate data in Portland, Oregon, USA. *Journal of Water and Climate Change*, 12(4), 1135–1153. <https://doi.org/10.2166/wcc.2020.043>

Davis, M., & Naumann, S. (2017). Making the case for sustainable urban drainage systems as a nature-based solution to urban flooding. In Kabisch, N., Korn, H., Stadler, J., & A., Bonn (Eds.), *Nature-Based Solutions to Climate Change Adaptation in Urban Areas. Theory and Practice of Urban Sustainability Transitions* (pp. 123–137). Springer. https://doi.org/10.1007/978-3-319-56091-5_8

Dharmarathne, G., Waduge, A.O., Bogahawaththa, M., Rathnayake, U., & Meddage, D.P.P. (2024). Adapting cities to the surge: A comprehensive review of climate-induced urban flooding. *Results in Engineering*, 22, 102123. <https://doi.org/10.1016/j.rineng.2024.102123>

Ekhout, J.P.C., & de Vente, J. (2022). Global impact of climate change on soil erosion and potential for adaptation through soil conservation. *Earth-Science Reviews*, 226, 103921. <https://doi.org/10.1016/j.earscirev.2022.103921>

Ettrichrätz, V., Beier, C., Keuler, K., & Trachte, K. (2023). Identification of regions with a robust increase of heavy precipitation events. *EGUsphere* [preprint].
<https://doi.org/10.5194/egusphere-2023-552>

Fuentes-Franco, R., Docquier, D., Koenigk, T., Zimmermann, K., & Giorgi, F. (2023). Winter heavy precipitation events over Northern Europe modulated by a weaker NAO variability by the end of the 21st century. *npj Climate and Atmospheric Science*, 6, 72.
<https://doi.org/10.1038/s41612-023-00396-1>

Gariano, S.L., & Guzzetti, F. (2016). Landslides in a changing climate. *Earth-Science Reviews*, 162, 227–252. <https://doi.org/10.1016/j.earscirev.2016.08.011>

Guerreiro, S.B., Glenis, V., Dawson, R.J., & Kilsby, C. (2017). Pluvial flooding in European cities - A continental approach to urban flood modelling. *Water*, 9(4), 296.
<https://doi.org/10.3390/w9040296>

Hurrell, J.W. (1995). Decadal trends in the North Atlantic Oscillation: Regional temperatures and precipitation. *Science*, 269, 676–679. 10.1126/science.269.5224.676

IPCC (2021). *Climate Change 2021: The Physical Science Basis. Contribution of Working Group I to the Sixth Assessment Report of the Intergovernmental Panel on Climate Change*. (Masson-Delmotte, V., Zhai, P., Pirani, A., Connors, S.L., Pean, C., Berger, S., Caud, N., Chen, Y., Goldfarb, L., Gomis, M.I., Huang, M., Leitzell, K., Lonnoy, E., Matthews, J.B.R., Maycock, T.K., Waterfield, T., Yelekci, O., Yu, R., & Zhou, B., Eds.). Cambridge University Press, Cambridge, United Kingdom and New York, NY, USA. <https://doi.org/10.1017/9781009157896>

Krichak, S.O., Breitgand, J.S., Gualdi, S.F., & Feldstein, S.B. (2014). Teleconnection-extreme precipitation relationships over the Mediterranean region. *Theoretical and Applied Climatology*, 117, 679–692. <https://doi.org/10.1007/s00704-013-1036-4>

Leščešen, I., Basarin, B., Pavić, D., & Mesaroš, M. (2023). Extreme Precipitation Analysis in Novi Sad. In Șerban, G., Horváth, C., Holobâcă, I., Bătinas, R., Tudose, T., Croitoru, A. (Eds.), *Proceedings of the Air and Water – Components of the Environment Conference* (pp. 140–147). Cluj-Napoca, Romania.
https://doi.org/10.24193/AWC2023_14

Malinović-Milićević, S., Mihailović, D.T., Radovanović, M.M., & Drešković, N. (2018). Extreme precipitation indices in Vojvodina region (Serbia). *Journal of the Geographical Institute Jovan Cvijić SASA*, 68(1), 1–15.
<https://doi.org/10.2298/IJGI1801001M>

Marchi, L., Borga, M., Preciso, E., & Gaume, E. (2010). Characterisation of selected extreme flash floods in Europe and implications for flood risk management. *Journal of Hydrology*, 394(1-2), 118–133. <https://doi.org/10.1016/j.jhydrol.2010.07.017>

May, R.M., Goebbert, K.H., Thielen, J.E., Leeman, J.R., Camron, M.D., Bruick, Z., Bruning, E.C., Manser, R.P., Arms, S.C., & Marsh, P.T. (2022). MetPy: A Meteorological Python Library for Data Analysis and Visualization. *Bulletin of the American Meteorological Society*, 103(10). <https://doi.org/10.1175/BAMS-D-21-0125.1>

Mehvar, S., Wijnberg, K., Borsje, B., Kerle, N., Schraagen, J. M., Vinke-de Kruijf, J., Geurs, K., Hartmann, A., Hogeboom, R., & Hulscher, S. (2021). Review article: Towards resilient vital infrastructure systems – challenges, opportunities, and future research

agenda. *Natural Hazards and Earth System Sciences*, 21, 1383–1407.
<https://doi.org/10.5194/nhess-21-1383-2021>

Milošević, D., Savić, S.M., Stojanović, V., & Popov-Raljić, J. (2015). Effects of precipitation and temperatures on crop yield variability in Vojvodina (Serbia). *Italian Journal of Agrometeorology*, 20(3), 35-46. https://www.agrometeorologia.it/wp-content/uploads/2024/06/2015_03_35-46_IJAm.pdf

Milošević, D., Savić, S., Kresoja, M., Lužanin, Z., Šećerov, I., Arsenović, D., Dunjić, J., & Matzarakis, A. (2022). Analysis of air temperature dynamics in the “local climate zones” of Novi Sad (Serbia) based on long-term database from an urban meteorological network. *International Journal of Biometeorology*, 66, 371-384.
<https://doi.org/10.1007/s00484-020-02058-w>

Mimić, G., Živaljević, B., Blagojević, D., Pejak, B., & Brdar, S. (2022). Quantifying the effects of drought using the crop moisture stress as an indicator of maize and sunflower yield reduction in Serbia. *Atmosphere*, 13(11), 1880.
<https://doi.org/10.3390/atmos13111880>

Patakamuri, S., & O'Brien, N. (2021). Modified Versions of Mann Kendall and Spearman's Rho Trend Tests. R package version 1.6. <https://CRAN.R-project.org/package=modifiedmk>

R Core Team (2023). A Language and Environment for Statistical Computing. R Foundation for Statistical Computing, Vienna, Austria. <https://www.R-project.org/>

Ruml, M., Gregorić, E., Vujadinović, M., Radovanović, S., Matović, G., Vuković, A., Počuća, V., & Stojićić, Dj. (2017). Observed changes of temperature extremes in Serbia over the period 1961–2010. *Atmospheric Research*, 183, 26–41.
<https://doi.org/10.1016/j.atmosres.2016.08.013>

Savić, S., Kalfayan, M., & Dolinaj, D. (2020). Precipitation Spatial Patterns in Cities with Different Urbanisation Types: Case Study of Novi Sad (Serbia) as a Medium-sized City. *Geographica Pannonica*, 24(2), 88–99. <https://doi.org/10.5937/gp24-25202>

Savić, S., Marković, V., Šećerov, I., Pavić, D., Arsenović, D., Milošević, D., ..., & Pantelić, M. (2018). Heat wave risk assessment and mapping in urban areas: case study for a midsized Central European city, Novi Sad (Serbia). *Natural Hazards*, 91, 891-911.
<https://doi.org/10.1007/s11069-017-3160-4>

Sounding, University of Wyoming. Available online:
<https://weather.uwyo.edu/upperair/sounding.html> (accessed on 9 November 2024).

Stosic, T., Tošić, M., Lazić, I., et al. (2024). Changes in rainfall seasonality in Serbia from 1961 to 2020. *Theoretical and Applied Climatology*, 155, 4123–4138.
<https://doi.org/10.1007/s00704-024-04871-4>

Sun, Q.X., Zwiers, F., Westra, S., & Alexander, L.V. (2021). A Global, Continental, and Regional Analysis of Changes in Extreme Precipitation. *Journal of Climate*, 34(1), 243–258. <https://doi.org/10.1175/JCLI-D-19-0892.1>

Tošić, I. (2004). Spatial and temporal variability of winter and summer precipitation over Serbia and Montenegro. *Theoretical and Applied Climatology*, 77, 47–56.
<https://doi.org/10.1007/s00704-003-0022-7>

Tošić, I., Hrnjak, I., Gavrilov, M.B., Unkašević, M., Marković, S.B., & Lukić, T. (2014) Annual and seasonal variability of precipitation in Vojvodina, Serbia. *Theoretical and Applied Climatology*, 117, 331-341. <https://doi.org/10.1007/s00704-013-1007-9>

Tošić, I., & Putniković, S. (2021). Influence of the East Atlantic/West Russia pattern on precipitation over Serbia. *Theoretical and Applied Climatology*, 146, 997–1006. <https://doi.org/10.1007/s00704-021-03777-9>

Tošić, I., Tošić, M., Lazić, I., Aleksandrov, N., Putniković, S., & Djurdjević, V. (2023) Spatio-temporal changes in the mean and extreme temperature indices for Serbia. *International Journal of Climatology*, 43(5), 2391–2410. <https://doi.org/10.1002/joc.798120>

Tošić, I., Unkašević, M., & Putniković, S. (2017). Extreme daily precipitation: the case of Serbia in 2014. *Theoretical and Applied Climatology*, 128, 785–794. <https://doi.org/10.1007/s00704-016-1749-2>

Trenberth, K.E. (1999). Conceptual framework for changes of extremes of the hydrological cycles with climate change. *Climatic Change*, 42, 327–339. <https://doi.org/10.1023/A:1005488920935>

Unger, J., Savić, S., & Gál, T. (2011) Modelling of the annual mean urban heat island pattern for planning of representative urban climate station network. *Advances in Meteorology*, 2011, 398613. <https://doi.org/10.1155/2011/398613>

van den Besselaar, E.J.M., Klein Tank, A.M.G., & Buishand, T.A. (2013). Trends in European precipitation extremes over 1951–2010. *International Journal of Climatology*, 33, 2682–2689. <https://doi.org/10.1002/joc.3619>

Vujadinović Mandić, M., Vuković Vimić, A., Ranković-Vasić, Z., Đurović, D., Ćosić, M., Sotonica, D., Nikolić, D., & Đurđević, V. (2022). Observed changes in climate conditions and weather-related risks in fruit and grape production in Serbia. *Atmosphere*, 13(6), 948. <https://doi.org/10.3390/atmos13060948>

Wang, X., Huang, G., & Liu, J. (2014). Projected increases in intensity and frequency of rainfall extremes through a regional climate modeling approach. *Journal of Geophysical Research: Atmospheres*, 119(23), 13271–13286. <https://doi.org/10.1002/2014JD022564>

Westra, S., Alexander, L.V., & Zwiers, F.W. (2013). Global increasing trends in annual maximum daily precipitation. *Journal of Climate*, 26(11), 3904–3918. <https://doi.org/10.1175/JCLI-D-12-00502.1>

Yang, Y., Ng, S.T., Zhou, S., Xu, F.J., & H. Li. (2020). Physics-based resilience assessment of interdependent civil infrastructure systems with condition-varying components: a case with stormwater drainage system and road transport system. *Sustainable Cities and Society*, 54, 101886. <https://doi.org/10.1016/j.scs.2019.101886>

Yin, H., & Sun, Y. (2018). Characteristics of extreme temperature and precipitation in China in 2017 based on ETCCDI indices. *Advances in Climate Change Research*, 9(4), 218–226. <https://doi.org/10.1016/j.accre.2019.01.001>

Yue, S., & Wang, C. (2004). The Mann-Kendall test modified by effective sample size to detect trend in serially correlated hydrological series. *Water Resources Management*, 18, 201–218. <https://doi.org/10.1023/B:WARM.0000043140.61082.60>

Zeder, J., & Fischer, E.M. (2020). Observed extreme precipitation trends and scaling in Central Europe. *Weather and Climate Extremes*, 29, 100266.
<https://doi.org/10.1016/j.wace.2020.100266>

Zhou, X., Bai, Z., & Yang, Y. (2017). Linking trends in urban extreme rainfall to urban flooding in China. *International Journal of Climatology*, 37(13), 4586–4593.
<https://doi.org/10.1002/joc.5107>